Novel mechanisms in murine nitrofen-induced pulmonary hypoplasia: FGF-10 rescue in culture

Juan M. Acosta, Bernard Thébaud, Carmenza Castillo, Arnaud Mailleux, Denise Tefft, Carol Wuenschell, Kathryn D. Anderson, Jacques Bourbon, Jean-Paul Thiery, Savério Bellusci and David Warburton

Novel mechanisms in murine nitrofen-induced pulmonary hypoplasia: FGF-10 rescue in culture

JUAN M. ACOSTA,[1,2,*] BERNARD THÉBAUD,[3–6,*] CARMENZA CASTILLO,[2]
ARNAUD MAILLEUX,[3] DENISE TEFFT,[2] CAROL WUENSCHELL,[2]
KATHRYN D. ANDERSON,[1] JACQUES BOURBON,[7] JEAN-PAUL THIERY,[3]
SAVÉRIO BELLUSCI,[3] AND DAVID WARBURTON[1–3]

[1]*Division of Pediatric Surgery and Developmental Biology Program, Childrens Hospital Los Angeles
Research Institute, Keck School of Medicine, University of Southern California, Los Angeles 90027;*
[2]*The Center for Craniofacial Molecular Biology, University of Southern California School of
Dentistry, Los Angeles, California 90033;* [3]*Equipe Morphogénèse Cellulaire et Progression Tumorale,
Institut Curie Unité Mixte de Recherche 144 Centre National de la Recherche Scientifique,
75005 Paris;* [4]*Service de Pédiatrie et Réanimation Néonatales-UPRES EA2704, Hôpital
Antoine Béclère, 92141 Clamart;* [5]*Service de Physiologie Respiratoire, Hôpital Cochin,
Université René Descartes, 75005 Paris;* [6]*Vascular Biology Research Group, University
of Alberta, Edmonton, Alberta T6G 2S2, Canada; and* [7]*Institut National de la Santé
et de la Recherche Médicale Unité 319, Universite Jussieu, 75005 Paris, France*

Acosta, Juan M., Bernard Thébaud, Carmenza
Castillo, Arnaud Mailleux, Denise Tefft, Carol Wuen-
schell, Kathryn D. Anderson, Jacques Bourbon, Jean-
Paul Thiery, Savério Bellusci, and David Warburton.
Novel mechanisms in murine nitrofen-induced pulmonary hy-
poplasia: FGF-10 rescue in culture. *Am J Physiol Lung Cell Mol
Physiol* 281: L250–L257, 2001.—We evaluated the role of the
key pulmonary morphogenetic gene fibroblast growth factor-10
(*Fgf10*) in murine nitrofen-induced primary lung hypoplasia,
which is evident before the time of diaphragm closure. In situ
hybridization and competitive RT-PCR revealed a profound
disturbance in the temporospatial pattern as well as a 10-fold
decrease in mRNA expression level of *Fgf10* but not of the induc-
ible inhibitor murine *Sprouty2 (mSpry2)* after nitrofen treat-
ment. Exogenous FGF-10 increased branching not only of con-
trol lungs [13% (right) and 27% (left); $P < 0.01$] but also of
nitrofen-exposed lungs [23% (right) and 77% (left); $P < 0.01$].
Expression of *mSpry2* increased 10-fold with FGF-10 in both
nitrofen-treated and control lungs, indicating intact downstream
FGF signaling mechanisms after nitrofen treatment. We con-
clude that nitrofen inhibits *Fgf10* expression, which is essential
for lung growth and branching. Exogenous FGF-10 not only
stimulates FGF signaling, marked by increased *mSpry2* expres-
sion, in both nitrofen-treated and control lungs but also sub-
stantially rescues nitrofen-induced lung hypoplasia in culture.

congenital diaphragmatic hernia; lung hypoplasia; fibroblast
growth factor-10; murine *Sprouty2*

CONGENITAL DIAPHRAGMATIC HERNIA (CDH) occurs in ~1 in
3,000 human live births. Although it is associated with

several genetic defects, its exact etiology is not known.
Newborns with CDH have a 40–50% mortality, which
is primarily caused by the associated pulmonary hy-
poplasia. The hypoplastic lungs are not capable of
providing adequate gas exchange for oxygenation, and
persistent pulmonary hypertension leads to refractory
hypoxia (right to left shunting). Unlike other causes of
neonatal respiratory failure, infants with CDH are
often unresponsive to the modern therapeutic arma-
mentarium because it does not solve the basic problem
of lung hypoplasia (28).

The hypoplastic lung in CDH is developmentally
delayed. There is a marked reduction from 21 genera-
tions of airways in the normal human lung to 12–14
generations in the ipsilateral and 16–18 generations in
the contralateral lung in CDH (1). There is also a delay
in the differentiation of alveolar epithelial cells, with a
resultant surfactant deficiency (31), and fewer and
more arterialized vascular branches (20). In addition to
the effect of mechanical compression by the herniated
abdominal viscera, lung hypoplasia in CDH may also
result from a primary abnormality in airway branching
(11, 15). However, the molecular mechanisms underly-
ing lung hypoplasia in human CDH have not been fully
investigated.

Since the first description of nitrofen-induced dia-
phragmatic hernias in rodents by Iritani (10) in 1984,
the murine nitrofen-induced model of CDH has been
extensively studied and by now is widely accepted as a
well-established model that has many phenotypic sim-
ilarities to the human condition (7, 16). Using this

1040-0605/01 $5.00 Copyright © 2001 the American Physiological Society

model in mice, we showed that nitrofen causes primary pulmonary hypoplasia, which is worsened by the presence of a hernia (4). In rats, nitrofen has also recently been shown to reduce branching morphogenesis before diaphragmatic closure both in vitro and in vivo (15). Because nitrofen-exposed embryonic lungs are clearly hypoplastic before the appearance of an actual diaphragmatic defect, we began to evaluate candidate factors known to be required for early lung development (30).

During mouse lung morphogenesis, the distal mesenchyme has long been known to regulate the growth and branching of the adjacent endoderm through the secretion of soluble factors [recently reviewed by Warburton et al. (30)]. Bellusci et al. (2) reported that fibroblast growth factor (FGF)-10 is a mesenchyme-derived factor that plays a critical role in patterning the early branching events in lung development. *Fgf10*-null mutant mice and transgenic mice expressing dominant negative forms of the FGF-10 receptor *Fgfr2-IIIb* have a dramatic inhibition of bronchial branching (19, 22). *Fgf10* is expressed in a temporospatially specific pattern in the peripheral embryonic lung mesenchyme near the positions where primary, secondary, and tertiary bronchi bud (2). The buds grow toward these areas of *Fgf10* expression. Thus *Fgf10* appears to stimulate and direct early bronchial branching. FGF pathway signaling is modified at each stage of branching by genetic feedback controls. *Sonic hedgehog* (*Shh*), which is strongly expressed in the distal epithelium, may function as a negative signal for *Fgf10* (3, 8). *Shh* inhibits *Fgf10* expression in the mesenchyme near the growing tips where the initial *Fgf10* expression domain splits laterally into two domains. Two new buds then sprout, each targeting one of the lateral subdomains of *Fgf10* expression. Mice in which *Shh* has been inactivated also have profound impairments of lung branching (21). Other key antagonists of the FGF pathway include members of the *Sprouty* gene family. Murine *Sprouty2* (*mSpry2*) is an inducible negative regulator of FGF receptor tyrosine kinase signaling that is expressed in the distal epithelium of the embryonic mouse lung adjacent to the mesenchymal loci of *Fgf10* expression at embryonic stages when the lung epithelial buds are highly responsive to FGF-10. Abrogation of *mSpry2* expression in lung organ cultures with antisense oligonucleotides increases branching morphogenesis and surfactant gene expression (27).

Here we determined that the temporospatial pattern of *Fgf10* expression in mouse embryonic lungs is severely disrupted in the presence of nitrofen-induced lung hypoplasia. Nevertheless, taking advantage of highly inducible *mSpry2* expression by FGF-10, we were able to determine that downstream FGF signaling was intact. We also determined that exogenous FGF-10 could increase branching morphogenesis in both wild-type and nitrofen-exposed embryonic lungs in culture. Thus nitrofen-induced lung hypoplasia may be at least partially explained by downregulation of *Fgf10*, whereas exogenous FGF-10 can substantially

rescue nitrofen-induced mouse embryonic lung hypoplasia in culture. These findings may have potential value in devising novel approaches to correcting lung hypoplasia in human CDH because only a small increase in diffusion capacity could be lifesaving.

MATERIALS AND METHODS

Nitrofen-exposed lungs. Timed-pregnant Swiss-Webster mice (Simonsen Laboratories, Gilroy, CA) were gavage fed 25 mg of nitrofen (2,4-dichlorophenyl-*p*-nitrophenyl ether; Radian International, Austin, TX) on *day 8* of gestation (presence of a vaginal plug = *day 0*). The control animals received olive oil. With the use of aseptic technique, the mouse embryos were harvested by cesarean section on embryonic *day* (ED) *12*. On retrieval, the embryos were transferred to an isotonic Hanks' balanced salt solution and cooled on ice. They were then microdissected from their extraembryonic membranes, and with the use of a stereomicroscope and microsurgical instruments, the lungs were excised and the right and left lobes were separated and placed in Hanks' balanced salt solution. The University of Southern California (Los Angeles, CA) Institutional Animal Care and Use Committee approved the use of animals in this study.

Whole mount in situ hybridization. The whole mount in situ hybridization technique was based on that previously described by Sasaki and Hogan (24). The following murine cDNAs were used as templates for synthesizing digoxin-labeled riboprobes: 584-bp FGF-10 and 948-bp full-length Spry2. To provide a qualitative comparison of levels of gene expression between control and nitrofen-exposed lungs between ED12 and ED15, the lungs were fixed and processed under the same conditions with respect to probe concentration and specific activity and washed at the same temperature and stringency. Photomicrographs were taken with the same exposure time.

Organ culture. ED12 lungs were cultured at the air-fluid interface by placing them on 0.8-μm MF-Millipore filters (Millipore, Bedford, MA) supported by stainless steel grids in culture dishes containing BGJb medium (GIBCO BRL, Life Technologies, Grand Island, NY) supplemented with 1 mg/ml of ascorbic acid and 50 U/ml of penicillin-streptomycin. FGF-10 was added to the culture medium at a concentration of 500 ng/ml (R&D Systems, Minneapolis, MN). FGF-10 is not very bioactive, and dose-response curves have demonstrated that at 500 ng/ml, there is the maximum amount of branching morphogenesis. Organ cultures were maintained at 37°C in 100% humidity and 95% air-5% carbon dioxide for 4 days, with the medium changed after 2 days.

Branching morphogenesis. Branching morphogenesis was quantified by counting the number of terminal branches visible around the periphery of each lung. This was performed before and after 4 days in culture with transillumination to visualize the structures and photomicrography to record permanent images (30a).

RNA extraction and reverse transcription. Individual cultured explants were homogenized by repeated pipetting in 4 M guanidinium isothiocyanate. Total RNA was then extracted with the Rapid Total RNA Isolation Kit (5 Prime → 3 Prime, Boulder, CO). Reverse transcription (RT) was performed by incubating samples of individual lung RNA at 37°C in 10 mM Tris (pH 8.4), 50 mM KCl, 2 mM $MgCl_2$, 1 mM dithiothreitol, 5 U of ribonuclease inhibitor, 0.5 mM deoxynucleotide triphosphates, 100 pmol of oligo(dT)$_{12-18}$, and 200 U of Moloney murine leukemia virus reverse transcriptase (USB, Cleveland, OH). The reaction was terminated by

heating for 5 min at 100°C. Reverse-transcribed products were then used for competitive PCR.

Competitive PCR. PCR amplification was performed with a DNA Robocycler (Stratagene, La Jolla, CA), with an initial denaturation at 94°C for 3 min followed by 35 cycles of denaturation at 93°C for 2 min, annealing at 62°C for 2 min, and extension at 72°C for 2 min. The final cycle concluded with a 5-min extension step. The reaction mixture contained 10 mM Tris (pH 8.4), 50 mM KCl, 2 mM $MgCl_2$ (optimized), 0.01% Triton X-100, 20 pmol of primer sets, 100 μM deoxynucleotide triphosphate, and 0.5 U of *Taq* thermostable DNA polymerase (Promega, Madison, WI). A reaction mixture containing 1 pg/μl of the appropriate competitor DNA was added to the reverse-transcribed samples derived from 50 ng of total RNA. The concentration of cDNA standard solutions was determined spectrophotometrically by absorbance at 260 nm. The equations drawn from the linear regressions for each of the standard curves were used to interpolate the mRNA amounts from their respective cDNA equivalents in each lung sample. To control for potential variations due to the efficiency of RNA extraction and RT, β-actin mRNA was also quantified in the same samples.

Competitive RT-PCR quantification. The same primers for mouse *mSpry2* were used to amplify both the cDNA and competitor for each gene of interest. The upstream primer of cDNA synthesis was 5′-TGTGAGGACTGTGGCAAGTGC-3′ and the downstream primer was 5′-TTTAAGGCAACCCTT-GCTGG-3′, resulting in a 300-bp PCR product. Two composite primers were synthesized to construct the *mSpry2* competitor. Each set of composite primers contained the *mSpry* sequence as well as a short sequence designed to hybridize to the cDNA of interest. This allowed the incorporation of the *mSpry2* sequence into the DNA during the PCR. The competitor was *v-erb*B DNA. The competitor was then sequenced to verify the incorporation of the gene-specific primers and was 400 bp long. The same primers were used to amplify 1 fg of competitor and scaled concentrations of cDNA. The log of cDNA/competitor was plotted against the target concentrations, producing a coefficient (r^2) > 0.98 (data not shown). The same assay was developed for *Fgf10*. Competitive PCR quantification allows accurate assessment of mRNA levels and is reliable without contaminating DNA species.

Electrophoresis and densitometric analysis. Target and competitor PCR products were separated by size with electrophoresis in 3% agarose gels (NuSieve, FMC BioProducts, Rockland, ME). Gels were stained with 5 μg/ml of ethidium bromide and photographed with a digital camera (Cohu, San Diego, CA). Band intensities were determined by densitometric analysis with ImageQuant band-analyzing software (Molecular Dynamics, Sunnyvale, CA). β-Actin mRNA levels were measured in an identical fashion in both groups as an internal control for RNA extraction and cDNA production. All mRNA values were normalized to β-actin mRNA levels, which were the same for nitrofen-exposed and control lungs.

Statistical analysis. Morphometric data are reported as means ± SD. Densitometric data are reported as the mean ratios of control values. Data from nitrofen-exposed lungs were compared with those of control lungs with two-tailed Student's *t*-test. A *P* value of <0.05 was considered significant.

RESULTS

Decreased temporospatial expression of Fgf10 in hypoplastic lungs. Fgf10 transcripts were studied during lung development by whole mount in situ hybridization. From ED12.5 through ED15.5, high levels of *Fgf10* expression were present in the mesenchyme adjacent to the epithelial buds of wild-type lungs (Fig. 1, *A* and *C*), correlating with the sites of future dichotomous branching. In contrast, in nitrofen-treated lungs, the temporospatial pattern expression of *Fgf10* was markedly impaired (Fig. 1*D*). Interestingly, loss of *Fgf10* expression appeared to correlate well with the severity of lung hypoplasia (Fig. 1*B*); *Fgf10* transcripts could be detected only in the caudal part of the left lobe in moderately severe hypoplasia (Fig. 1*F*), whereas expression was nearly totally abolished in examples with more severe hypoplasia (Fig. 1*E*).

Whole mount in situ hybridization localized *mSpry2* expression in the distal epithelium from ED12.5 to ED15.5 in normal lungs (Fig. 2, *A* and *B*). In nitrofen-exposed lungs, *mSpry2* seemed to be less expressed at ED12.5 (Fig. 2, *A* and *E*), but from ED13.5 to ED15.5, *mSpry2* was expressed normally at the distal tips of epithelial buds (Fig. 2, *C*, *D*, and *F–H*).

Nitrofen exposure, FGF-10, and relative mRNA expression of Fgf10 and mSpry2. Fgf10 and *mSpry2* expression levels were measured by competitive RT-PCR and compared between wild-type and nitrofen-exposed and between right and left ED12 lungs after 4 days in culture. The results of this analysis are shown in Figs. 3 and 4 and were all corrected as ratios to β-*actin* mRNA. The mean ratios of *Fgf10* to β-*actin* expression were 2.65 in the right and 1.26 in the left wild-type lungs. These relative levels of expression decreased to 0.4 (right) and 0.3 (left) after exposure to exogenous FGF-10 (all *P* < 0.05). It is also interesting to note that *Fgf10* mRNA levels were reduced significantly after in utero exposure to nitrofen in both the right and left lungs. On the other hand, the mean level of expression of *mSpry2* mRNA did not differ significantly between the right and left lungs in wild-type or nitrofen-exposed embryos. However, levels of *mSpry2* expression did increase 4- to 10-fold in the presence of exogenous *Fgf10* under all conditions examined.

Nitrofen exposure, lung branching morphogenesis, and FGF-10 rescue. Nitrofen exposure produced a profound decrease in branching morphogenesis, which was already evident at ED12 and persisted when ED12 lungs were cultured for 4 days, as illustrated in Fig. 5 and quantified in Fig. 6. Nitrofen exposure resulted in an almost complete arrest of lung budding in the left lung (Fig. 5*B*). The effects on branching in the right lung were also very striking; budding over 4 days in culture was very significantly decreased in the right lungs after nitrofen exposure (Fig. 5*A*).

Exogenous FGF-10 produced a very striking and significant increase in overall size, lumen size, and branch numbers during morphogenesis in wild-type control ED12 lungs over 4 days in culture (Fig. 7). FGF-10 also produced a significant increase in the size and complexity of ED12 nitrofen-exposed lungs over 4 days in culture (Fig. 5). However, although the proportional increase in branch numbers was the same as in the wild type, the final number of branches in the nitrofen-exposed lungs was less than in the wild type, probably because of the relatively smaller starting
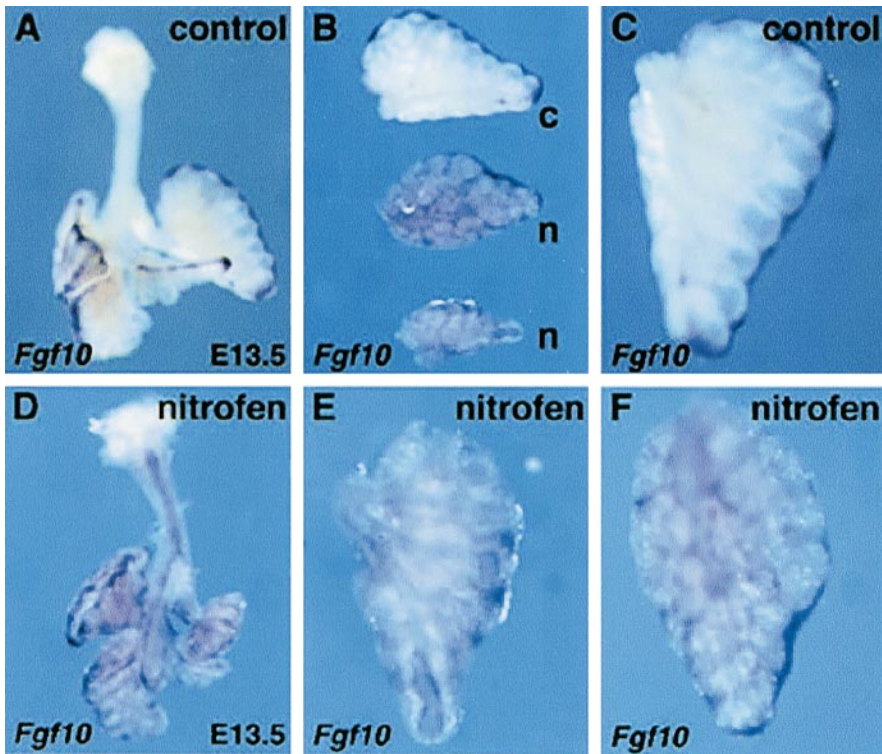
Fig. 1. Fibroblast growth factor-10 (*Fgf10*) expression in control and nitrofen-exposed mouse embryonic lungs detected by whole mount in situ hybridization on embryonic *day* (E) *13.5*. Note high levels of *Fgf10* expression present in the mesenchyme adjacent to the epithelial buds of control lungs (*A*) and at higher magnification in the left lobe of a control lung (*C*), correlating with the sites of future dichotomous branching. The hypoplastic nitrofen (n)-exposed lung shows profound disturbances in the temporospatial expression of *Fgf10* (*B–F*) compared with control (c). *Fgf10* transcripts were detected only in the caudal part of the left lobe (*F*). *Fgf10* expression was nearly totally abolished in a more severe hypoplastic left lobe (*E*).

number. However, the gains in branching with FGF-10 after nitrofen exposure were important, with the right lung restored to the same number of branches as the wild-type lungs grown without the benefit of FGF-10, whereas the numbers of branches in the left lung increased by 77%.

The number of lungs placed in culture was 25 right and 20 left control lungs, 25 right and 20 left control plus FGF-10 (500 ng/ml)-treated lungs, 25 right and 15 left nitrofen-exposed lungs, and 25 right and 20 left nitrofen-exposed plus FGF-10 (500 ng/ml)-treated lungs.

DISCUSSION

Nitrofen-induced early lung hypoplasia that occurs before closure of the diaphragm and that persists for
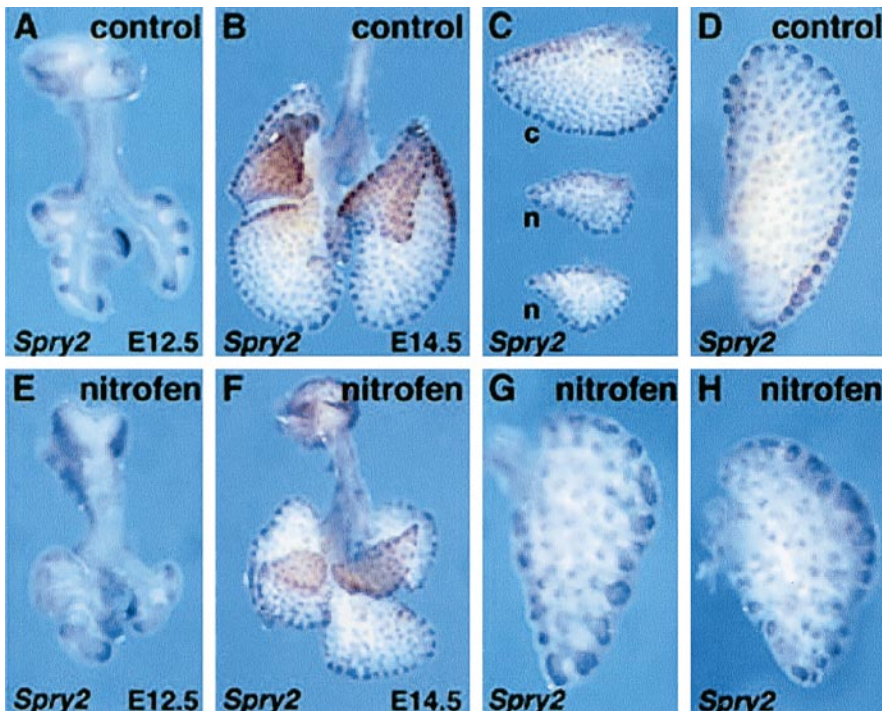

Fig. 2. Murine *Sprouty2* (*Spry2*) expression in control and nitrofen-exposed mouse embryonic lungs detected by whole mount in situ hybridization. On E12.5, *mSpry2* expression was slightly less expressed in the distal tips of the epithelium (*A* and *E*). *mSpry2*, localized to the distal tips of the epithelial buds, is equally expressed in control (*B* and *D*) and nitrofen-exposed (*C* and *F–H*) lungs on E14.5.
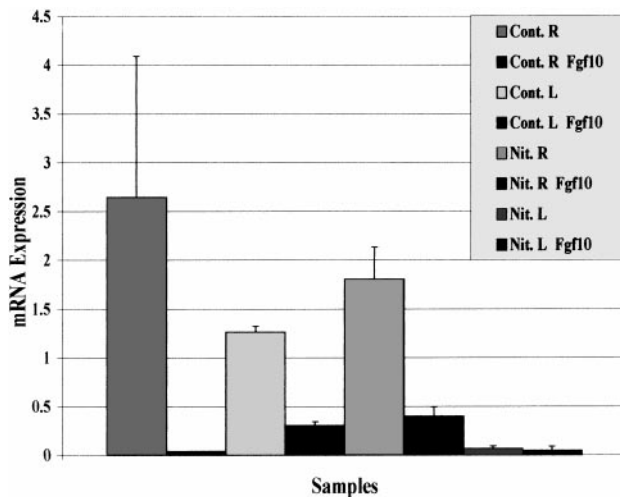
Fig. 3. Mean ratios of *Fgf10* expression relative to *β-actin* were 2.65 in right (R) and 1.26 in left (L) wild-type lungs. Results were all corrected as ratios to *β-actin* mRNA. These levels of expression decreased respectively to 0.04 (right) and 0.3 (left) after placement of exogenous *Fgf10* (all $P < 0.05$). In the nitrofen (Nit)-exposed lungs, the expression in the right lung was 1.80, which decreased to 0.40 after placement of exogenous *Fgf10* ($P < 0.05$). Expression in the left lung was 0.067 and decreased to 0.046 after placement of exogenous *Fgf10* (no statistical difference). Cont, control.

up to 72 h in culture was recently reported in the rat model (11). Here we showed that this is also the case in the mouse. However, in contrast to the rat, where the incidence of hypoplasia and CDH is reported to be the same at ~36%, Coleman et al. (4) and Iritani (10) found that hypoplasia occurs in >90% of mice, whereas the incidence of CDH is about half that in the rat. Thus, as Coleman et al. (4) have reported before, nitrofen-induced lung hypoplasia does not predict which mice will get CDH, but the degree of hypoplasia is greatly exacerbated by the presence of an ipsilateral CDH. This has recently been referred to by Keijzer et al. (15) as the two-hit hypothesis. In the present study, we
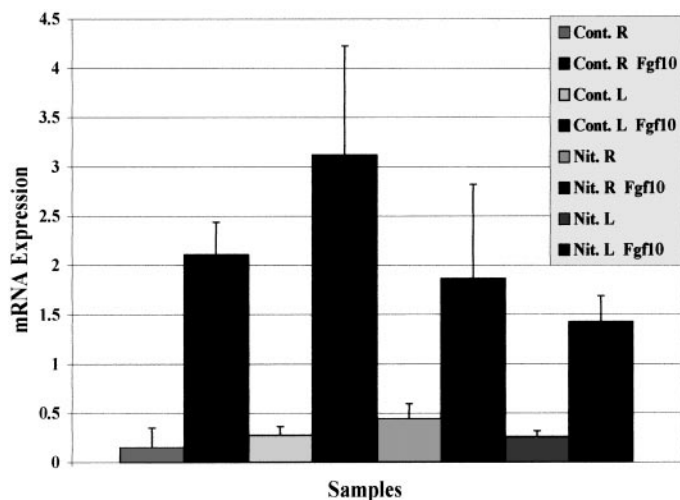

Fig. 4. Levels of *Spry2* mRNA expression increased 4- to 10-fold in the presence of exogenous *Fgf10* under all conditions examined. Results were all corrected as ratios to *β-actin* mRNA.
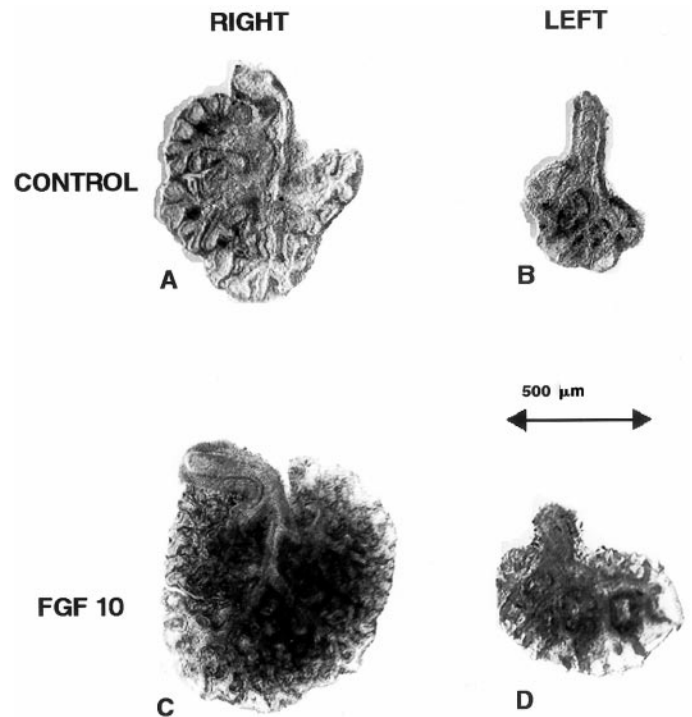

Fig. 5. FGF-10 rescues nitrofen-induced lung hypoplasia on the right side. *A*: nitrofen-exposed right lung (average of 43.2 terminal branches). *B*: nitrofen-exposed left lung (average of 11.1 terminal branches). *C*: nitrofen-exposed right lung with FGF-10 (500 ng/ml; average of 52.9 terminal branches). *D*: nitrofen-exposed left lung with FGF-10 (500 ng/ml; average of 19.7 terminal branches).

killed our mice on ED12 so we can only comment here on the primary lung hypoplasia induced by nitrofen, which has recently been reported to be associated with decreased cell proliferation (12).

The temporospatial pattern of *Fgf10* expression in the wild-type murine embryonic lung supports the concept that FGF-10 plays a key role in the directional outgrowth and possibly the induction of epithelial buds. By using whole mount in situ hybridization and competitive RT-PCR, we show that *Fgf10* mRNA expression is severely temporospatially disrupted and significantly decreased in nitrofen-exposed lungs compared with that in control lungs. We further show that exogenous FGF-10 induces significant lung growth by stimulating lung branching morphogenesis in both control and nitrofen-exposed lungs in culture. These observations suggest that abnormal FGF-10 signaling may account substantially for the decreased branching in nitrofen-induced lung hypoplasia before the onset of CDH.

Jesudason et al. (13) recently worked with FGF-1 and FGF-2 and also concluded that there is an intrinsic abnormality of the FGF signaling system in hypoplastic lungs after nitrofen treatment. However, an important caveat is that decreased expression and/or function of several other key morphogenetic genes has been reported previously in this model. These include thyroid transcription factor-1 (17), endothelin-converting enzyme neutral endopeptidase (14), basic FGF, plate-

Right Lung Branching
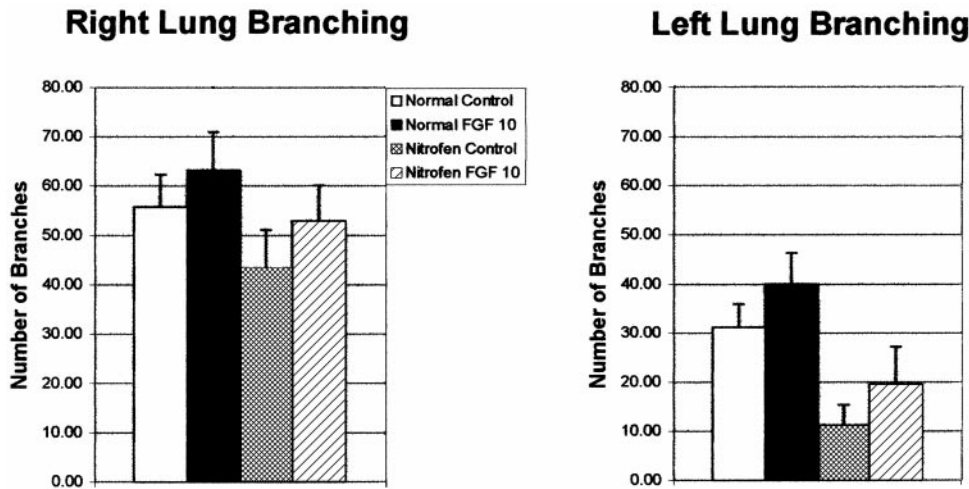

Left Lung Branching

Fig. 6. Branching morphogenesis in control and nitrofen-exposed lungs with and without FGF-10. Right control lungs showed a 13% increase in branching with exogenous FGF-10 ($P < 0.01$). Nitrofen-exposed right lungs demonstrated a 22% increase in branching ($P < 0.01$). Control left lungs showed a 28% increase with exogenous FGF-10 ($P < 0.01$). Nitrofen-exposed left lungs demonstrated a 77% increase in branching ($P < 0.01$).

let-derived growth factor (9), and tumor necrosis factor-α (25, 26).

We think that some of the most attractive pieces of data supporting a unifying theory that nitrofen-induced lung hypoplasia is caused by abnormalities of *Fgf10* expression are as follows: *1*) *Fgf10* signaling is clearly necessary for lung morphogenesis distal to the trachea because null mutation of *Fgf10* completely abrogates this process (19); *2*) many of the associated tracheobronchial and skeletal abnormalities caused by nitrofen exposure, including skull hypoplasia, axial appendicular, and rib anomalies, can also result from abnormalities in the FGF receptor signaling pathway (18, 32); and *3*) the findings reported herein, that

exogenous FGF-10 both stimulates wild-type lung morphogenesis and substantially rescues nitrofen-induced embryonic lung hypoplasia in culture, further support the concept that nitrofen may interfere with *Fgf10* expression. It seems unlikely that nitrofen interferes with downstream FGF-10 signaling because *mSpry2* expression was still induced normally in the presence of exogenous FGF-10 in nitrofen-exposed embryonic lungs in culture. However, *mSpry2* may also play a role in nitrofen-induced lung hypoplasia because its expression level remains unchanged, allowing relative accumulation of this negative regulator in excess of available FGF-10. On the other hand, the brisk induction of *mSpry2* expression by exogenous FGF-10 in both wild-
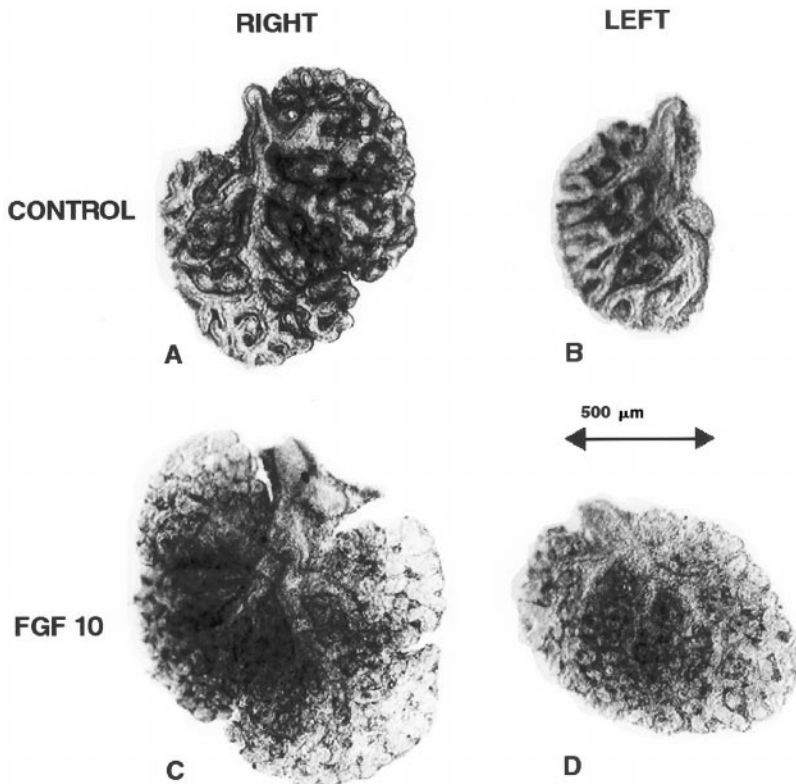

Fig. 7. FGF-10 increases branching morphogenesis in control lungs. *A*: right lung control (average of 55.7 terminal branches). *B*: left lung control (average of 31.2 terminal branches). *C*: right lung with FGF-10 (500 ng/ml; average of 63.2 terminal branches). *D*: left lung with FGF-10 (500 ng/ml; average of 39.9 terminal branches).

type and nitrofen-exposed lungs indicates that FGF signaling can still activate *mSpry2* even in the presence of nitrofen-induced hypoplasia. Thus *mSpry2* probably functions normally as a readily inducible negative modulator of FGF signaling even in the presence of nitrofen-induced hypoplasia.

Previous experimental approaches for rescuing lung hypoplasia associated with nitrofen exposure and CDH have included tracheal ligation and glucocorticoid, retinoid, and antioxidant treatment. Tracheal ligation certainly does increase the overall size and wet weight of the murine embryonic lung in culture, as it does when carried out in utero in sheep and also in humans (6). One rationale behind tracheal ligation is that it traps tracheal effluent, which is driven by active chloride secretion during embryonic and fetal life, thereby expanding the epithelial surface by positive hydraulic pressure. However, as recently reported (6), mesenchymal and epithelial maturation in the lung does not proceed normally under these conditions, and therapeutic results in humans have, for the most part, been disappointing. Glucocorticoids, on the other hand, are now considered a standard of care as preventive therapy to accelerate lung maturation in human premature labor (5). They have been reported to have many possible beneficial effects in the nitrofen model, most notably with respect to the current study, by inducing the expression of several peptide growth factors including FGF and platelet-derived growth factor. However, the effects of tracheal ligation and/or glucocorticoids may have negative consequences on postnatal alveolar development. Retinoids, on the other hand, appear to decrease the incidence and severity of nitrofen-induced CDH and may even have beneficial effects on alveolarization (23, 29).

Here we show for the first time that nitrofen-induced embryonic mouse lung hypoplasia is associated with decreased and temporospatially abnormal expression of *Fgf10*. Finally, nitrofen-induced lung hypoplasia is present on ED12, is worse in the left than in the right lung, persists in embryonic lung culture, and, most importantly, can be substantially rescued in culture by exogenous FGF-10. Taken together, these results lead us to speculate that nitrofen-induced lung hypoplasia may be caused, at least in part, by abnormalities in *Fgf10* expression. Furthermore, we speculate that novel therapeutic approaches designed to achieve either direct or indirect correction of FGF-10 signaling may, in the future, have the potential to contribute to the substantial rescue of in utero lung hypoplasia as seen in human neonates with CDH.

REFERENCES

1. **Areechnon W and Reid L.** Hypoplasia of lung with congenital diaphragmatic hernia. *Br Med J* 1: 230–233, 1963.
2. **Bellusci S, Grindley J, Emoto H, Itoh N, and Hogan BL.** Fibroblast growth factor 10 (FGF10) and branching morphogenesis in the embryonic mouse lung. *Development* 124: 4867–4878, 1997.
3. **Bellusci S, Yasuhide F, Rush MG, Henderson R, Winnier G, and Hogan BL.** Involvement of Sonic hedgehog (Shh) in mouse embryonic lung growth and morphogenesis. *Development* 124: 53–63, 1997.
4. **Coleman C, Zhao J, Gupta M, Buckley S, Tefft JD, Wuenschell CW, Minoo P, Anderson KD, and Warburton D.** Inhibition of vascular and epithelial differentiation in murine nitrofen-induced diaphragmatic hernia. *Am J Physiol Lung Cell Mol Physiol* 274: L636–L646, 1998.
5. **Crowley P.** Prophylactic corticosteroids for preterm birth (Cochrane Review). In: *The Cochrane Library*. Oxford, UK: Update Software, 2000, issue 4.
6. **Flake AW.** Fetal surgery for congenital diaphragmatic hernia. *Semin Pediatr Surg* 5: 266–274, 1996.
7. **Greer JJ, Allan DW, Babiuk RP, and Lemke RP.** Recent advances in understanding the pathogenesis of nitrofen-induced congenital diaphragmatic hernia. *Pediatr Pulmonol* 29: 394–399, 2000.
8. **Grindley JC, Bellusci S, Perkins D, and Hogan BL.** Evidence for the involvement of the Gli gene family in embryonic mouse lung development. *Dev Biol* 188: 337–348, 1997.
9. **Guarino N, Shima H, and Puri P.** The hypoplastic heart in congenital diaphragmatic hernia: reduced expression of basic fibroblast growth factor and platelet-derived growth factor. *Pediatr Surg Int* 16: 243–246, 2000.
10. **Iritani I.** Experimental study on embryogenesis of congenital diaphragmatic hernia. *Anat Embryol (Berl)* 169: 133–139, 1984.
11. **Jesudason EC, Connell MG, Fernig DG, Lloyd DA, and Losty PD.** Early lung malformations in congenital diaphragmatic hernia. *J Pediatr Surg* 35: 124–127, 2000.
12. **Jesudason EC, Connell MG, Fernig DG, Lloyd DA, and Losty PD.** Cell proliferation and apoptosis in experimental lung hypoplasia. *J Pediatr Surg* 35: 129–133, 2000.
13. **Jesudason EC, Connell MG, Fernig DG, Lloyd DA, and Losty PD.** In vitro effects of growth factors on lung hypoplasia in a model of congenital diaphragmatic hernia. *J Pediatr Surg* 35: 914–922, 2000.
14. **Kavanagh M, Battistini B, Kluth D, Jean S, Fournier L, Jeng AY, Major D, and Cloutier R.** Effects of CGS 26303, an endothelin-converting enzyme-neutral endopeptidase inhibitor, on nitrofen-induced congenital diaphragmatic hernia in the rat. *J Pediatr Surg* 35: 780–784, 2000.
15. **Keijzer R, Liu J, Deimling J, Tibboel D, and Post M.** Dual-hit hypothesis explains pulmonary hypoplasia in the nitrofen model of congenital diaphragmatic hernia. *Am J Pathol* 156: 1299–1306, 2000.
16. **Kluth D, Kangah R, Reich P, Tenbrinck R, Tibboel D, and Lambrecht W.** Nitrofen-induced diaphragmatic hernias in rats: an animal model. *J Pediatr Surg* 25: 850–854, 1990.
17. **Losada A, Xia H, Migliazza L, Diez-Pardo JA, Santiesteban P, and Tovar JA.** Lung hypoplasia caused by nitrofen is mediated by down-regulation of thyroid transcription factor (TTF-1). *Pediatr Surg Int* 15: 188–191, 1999.
18. **Migliazza L, Xia H, Diez-Pardo JA, and Tovar JA.** Skeletal malformations associated with congenital diaphragmatic hernia: experimental and human studies. *J Pediatr Surg* 34: 1624–1629, 1999.
19. **Min H, Danilenko DM, Scully SA, Bolon B, Ring BD, Tarpley JE, DeRose M, and Simonet WS.** Fgf-10 is required for both limb and lung development and exhibits striking functional similarity to *Drosophila* branchless. *Genes Dev* 12: 3156–3161, 1998.
20. **O'Toole SJ, Irish MS, Holm BA, and Glick PL.** Pulmonary vascular abnormalities in congenital diaphragmatic hernia. *Clin Perinatol* 23: 781–794, 1996.

21. **Pepicelli CV, Levis PM, and MacMahon AP.** Sonic hedgehog regulates lung branching morphogenesis in the mammalian lung. *Curr Biol* 8: 1083–1086, 1998.
22. **Peters K, Werner S, Liao X, Wert S, Whitsett J, and Williams L.** Targeted expression of a dominant negative FGF receptor blocks branching morphogenesis and epithelial differentiation of the mouse lung. *EMBO J* 13: 3296–3301, 1994.
23. **Pierce RA and Shipley JM.** Retinoid-enhanced alveolization: identifying relevant downstream targets. *Am J Respir Cell Mol Biol* 23: 137–141, 2000.
24. **Sasaki H and Hogan BLM.** Differential gene expression of multiple fork head related genes during gastrulation and axial pattern formation in the mouse embryo. *Development* 9: 2105–2116, 1995.
25. **Shima H, Oshiro K, Taira Y, Miyazaki E, Oue T, and Puri P.** Antenatal dexamethasone suppresses tumor necrosis factor-alpha expression in hypoplastic lung in nitrofen-induced diaphragmatic hernia in rats. *Pediatr Res* 46: 633–637, 1999.
26. **Shima H, Oue T, Taira Y, Miyazaki E, and Puri P.** Antenatal dexamethasone enhances endothelin receptor B expression in hypoplastic lungs in nitrofen-induced diaphragmatic hernia in rats. *J Pediatr Surg* 35: 203–207, 2000.
27. **Tefft JD, Lee M, Smith S, Leinwand M, Zhao J, Bringas P Jr, Crowe DL, and Warburton D.** Conserved function of mSpry-2, a murine homolog of *Drosophila* sprouty, which nega-

tively modulates respiratory organogenesis. *Curr Biol* 9: 219–222, 1999.
28. **Thébaud B, Mercier JC, and Dinh-Xuan AT.** Congenital diaphragmatic hernia: a cause of persistent pulmonary hypertension which lacks an effective therapy. *Biol Neonate* 74: 323–336, 1998.
29. **Thébaud B, Tibboel D, Rambaud C, Mercier J-C, Bourbon JR, Dinh-Xuan AT, and Archer SL.** Vitamin A decreases the incidence and severity of nitrofen-induced diaphragmatic hernias in rats. *Am J Physiol Lung Cell Mol Physiol* 277: L423–L429, 1999.
30. **Warburton D, Schwarz M, Tefft D, Flores-Delgado G, Anderson KD, and Cardoso WV.** The molecular basis of lung morphogenesis. *Mech Dev* 92: 55–81, 2000.
30a. **Warburton D, Seth R, Shum L, Horcher P, Hall FL, Werb Z, and Slaukin HC.** Epigenetic role of epidermal growth factor signalling in the regulation of embryonic lung morphogenesis. *Dev Biol* 149: 123–129, 1992.
31. **Wilcox DT, Irish MS, Holm BA, and Glick PL.** Pulmonary parenchymal abnormalities in congenital diaphragmatic hernia. *Clin Perinatol* 23: 771–779, 1996.
32. **Xia H, Migliazza L, Diez-Pardo JA, and Tovar JA.** The tracheobronchial tree is abnormal in experimental congenital diaphragmatic hernia. *Pediatr Surg Int* 15: 184–187, 1999.